Performance Characterization of GISMO, a 2 Millimeter TES Bolometer Camera used at the IRAM 30 m Telescope

Johannes G. Staguhn[1,2,*], Dominic J. Benford[1], Christine A. Allen [1], Stephen F. Maher [1,3], Elmer H. Sharp [1,4], Troy J. Ames[1], Richard G. Arendt[1] , David T. Chuss[1], Eli Dwek[1], Dale J. Fixsen[1,2], Tim M. Miller[1,5], S. Harvey Moseley[1], Santiago Navarro[6], Albrecht Sievers[6], Edward J.Wollack[1]

[1]*NASA/Goddard Space Flight Center, Greenbelt, MD 20771, USA;*

[2]*Dept. of Astronomy, University of Maryland, College Park, MD 20742, USA;*

[3]*Science Systems &: Applications, 10210 Greenbelt Rd. Ste. 600, Lanham, MD 20706, USA;*

[4]*Global Science & Technology: 7855 Walker Drive, Ste 200, Greenbelt, MD 20770 , USA;*

[5]*MEI Technologies, 7404 Executive Place, Suite 500, Seabrook, MD 20706, USA;*

[6]*IRAM, Avenida Divina Pastora, 7, Nucleo Central, E 18012 Granada, Spain;*

* Contact: Johannes.G.Staguhn@nasa.gov, phone +1-301-286-7840

Abstract— The 2mm spectral range provides a unique terrestrial window enabling ground-based observations of the earliest active dusty galaxies in the universe and thereby allowing a better constraint on the star formation rate in these objects. In November, 2007 we have fielded our 2mm bolometer camera GISMO (the Goddard IRAM Superconducting 2 Millimeter Observer) at the IRAM 30m telescope on Pico Veleta in Spain. GISMO uses a monolithic 8x16 Backshort-Under-Grid array with integrated TES detectors with 2 mm-pitch. We will present early results from our observing run with the first fielded BUG bolometer array.

I. Introduction

Our team has been building a 2 millimeter wavelength bolometer camera, the Goddard-IRAM Superconducting 2 Millimeter Observer (GISMO) for astronomical observations at the IRAM 30 m telescope on Pico Veleta, Spain [1]. The camera uses an 8×16 array of close-packed, high sensitivity, transition edge sensor (TES) bolometers with a pixel size of 2×2 mm^2, which was built in the Detector Development Laboratory at NASA/GSFC. The superconducting bolometers are read out by SQUID time domain multiplexers from NIST/Boulder [2]. In order to permit background-limited observations in the 2 mm atmospheric window at Pico Veleta, the required sensitivity expressed in Noise Equivalent Power (NEP) for the detectors is ~ $4 \cdot 10^{-17}$ W/sqrt(Hz) [3]. The array architecture we use is based on the Backshort Under Grid (BUG) design [4], which consists of three components: 1) a TES-based bolometer array with background-limited sensitivity and high filling factor, 2) a quarter-wave reflective backshort grid providing high optical efficiency, and 3) a superconducting bump-bonded large format Superconducting Quantum Interference Device (SQUID) multiplexer readout. This design is scalable to kilopixel size arrays for future ground-based, suborbital and space-based X-ray and far-infrared through millimeter cameras. The GISMO instrument is optimized for large area sky surveys, and it is most efficient at the detection of dusty galaxies at very high redshifts. High sensitivity observations will even be possible in the summer season. We performed a first engineering field test of GISMO at the 30 m telescope in November 2007.

II. Scientific Motivation

Due to the low background emission of the Earth's atmosphere at a wavelength of 2 millimeters, astronomical observations in this atmospheric window are efficient for the detection of the earliest active dusty galaxies in the universe [5]. Continuum measurements of galaxies at 2 mm wavelength are well-suited to determine the star formation rate and the total energy output in these objects. These 2 mm observations will complement existing SEDs of high redshift galaxies in the Rayleigh-Jeans part of the dust emission spectrum, even at the highest redshifts. At Pico Veleta, the site of the IRAM 30 m Telescope, the atmospheric photon noise at 2 mm is about a factor of three lower than it is at 1.2 mm wavelength. As a consequence, at redshifts of $z > 5$, sky background limited bolometric observations at 2 mm are highly efficient as compared to observations at shorter (sub-)millimeter wavelengths [5].

III. The GISMO Instrument

A. Dewar and Optics

GISMO is a bolometer camera intended specifically to maximize the likelihood of detecting large numbers of very high redshift galaxies. We designed fast f/1.2 optics for an approximately 0.9 λ/D sampling, intended to optimize the

efficiency of GISMO for large area blank sky surveys, yet without compromising the achievable point source signal-to-noise ratio [6]. A 4 inch (100 mm) diameter, anti-reflection coated, silicon lens provides the required focal ratio, and is cooled to 4.2 K to reduce the background on the detector. The cryostat is designed as a straightforward, simple-to-operate system with no moving parts. The instrument has a combination of ^{4}He and ^{3}He evaporation coolers that are pocketed into the dewar cold plate, providing a base temperature of 260 mK for the detector array. A more detailed description of the instrument design can be found in [7]. The detector arrays are read out by four 32-channel SQUID multiplexers, manufactured by NIST/Boulder [2]. Both the readout electronics and the instrument remote control and data acquisition software are presently being used in other instruments, such as the Green Bank Telescope 3 mm bolometer camera MUSTANG. [8]. GISMO is designed as a very simple instrument targeted at producing the maximum scientific return for the minimum investment in time.

B. Detectors

GISMO is enabled by a new detector technology developed by the Detector Development Laboratory (DDL) at the NASA/Goddard Space Flight Center. We have an ongoing program to develop several key technologies necessary to build kilopixel arrays in the BUG architecture [9]. The arrays consist of TES-based bolometers with resonant backshorts and SQUID Multiplexer readouts The detector architecture has advanced to the point that we can now produce 8×16 pixel arrays of 2 mm pitch bolometers for GISMO (Figure 1).

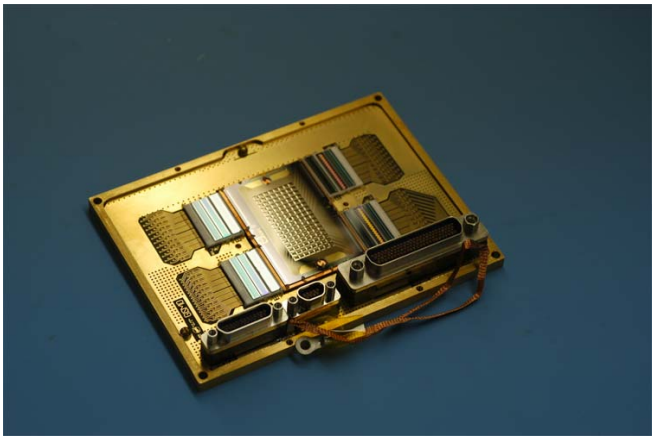

Fig. 1 The GISMO 8x16 planar array in the detector package. SQUID multiplexers, shunts and Nyquist inductors are integrated in the package

The array is a filled square grid of micromachined bolometers on a 1μm silicon membrane having superconducting TES bilayers and infrared absorbing films. The absorber is directly deposited onto the suspended bolometer, and is tuned to have an electrical resistivity of 400 Ω/square at 400mK. The coating for GISMO is bismuth, protected with a layer of silicon monoxide, to slow the adsorption of atmospheric water vapor into the bismuth during handling. To optimize the optical efficiency a λ/4 backshort (in the case of GISMO a reflective backshort) is placed a distance of 0.5 mm behind the detectors. This, coincidentally, is the thickness of the silicon-on-insulator support wafer upon which the detectors are fabricated, making it a simple matter to mount the detector chip on a reflective surface, in our case a copper-coated alumina board, to serve as the back-short. We use a normal metal "Zebra" stripe structure on the TES devices, which is used to suppress excess noise [10] and indeed provides near fundamental-noise-limited performance of the devices [11].

IV. INSTRUMENT PERFORMANCE AT THE TELESCOPE

Here we present early demonstration results from our first observing run at the IRAM 30 m Telescope, Nov. 5 -13, 2007 (Fig. 2, left). GISMO was mounted at the position of the MAMBO-II 1.2 mm bolometer camera [12] (Fig. 2, right).

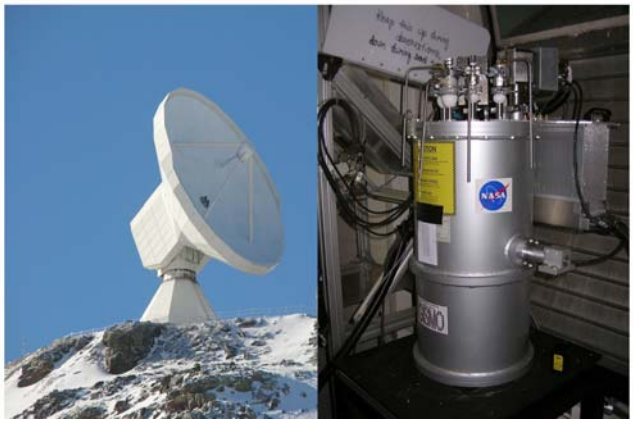

Fig. 2 *Left:* the IRAM 30m Telescope on Pico Veleta, Spain. *Right:* the GISMO dewar at the IRAM 30m telescope

In order to accommodate all weather conditions for this observing run we used a 40% transmission neutral density filter, which is mounted in front of the detector package. The filter allows for sky temperatures up to 150 K without saturating the TESs (which have a saturation power of ~ 35 pW). Once installed, we observed a beam spillover which manifested itself as radiation picked up from the mirror mount of the first fixed flat mirror in the 30m receiver cabin. This spillover, which we had not detected in the laboratory, is likely the result of the cold baffles in GISMO being slightly undersized (a deficiency we are in the process of fixing for the next observing run), and a minor misalignment of one of our non-planar mirrors during the installation at the telescope. For the observing run we therefore had to build a warm field stop that was mounted in front of the cryostat window, which is oversized by 20% in diameter. As a result of this warm stop we estimate that the effective detected background photon noise level was increased by several Kelvin. After a quick optical pre-alignment with a laser we pointed the instrument to the sky where we immediately detected the planets Jupiter and Mars, both of which, as expected, saturated our detectors. Fig. 3 shows three raw noise spectra we observed towards the sky: Two of those

(darker grey) are averages from working pixels, while the light grey dots shows the observed spectrum from an average of pixels in the "dead quadrant", a quadrant of the array we had lost the ability to bias the detectors due to the liftoff of the wire bonds for the detector bias, i.e. the detectors in this quadrant were regular superconductors.

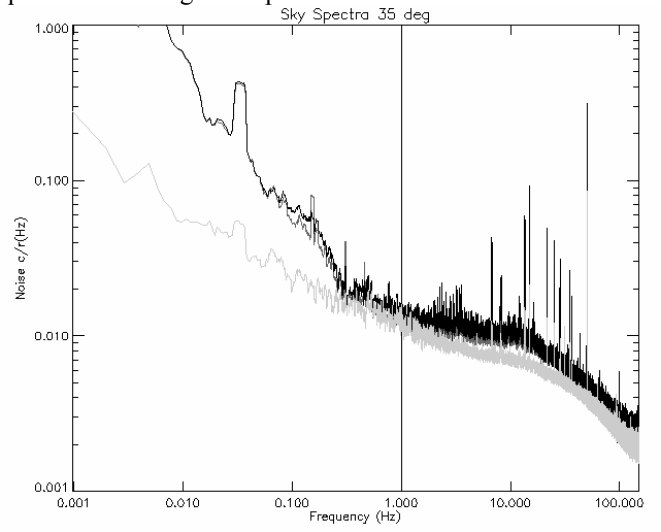

Fig. 3 Raw spectra of detector current noise density of GISMO while installed at the telescope and looking at the sky (dark and medium dark grey: average spectra of working pixels; light grey: average noise spectrum of superconducting (i.e. non biased) detectors

Note the wide range of the time axis, which ranges from 1 mHz - or 17 minutes - to 100 Hz. Many important features are visible in the plot: 1) The underlying 1/f properties of the readout (note that the drop-off beyond 10 Hz is due to feedback algorithm) is common to all three pixels. 2) Sky temperature variations are detected by the working pixels and dominate the noise at about 0.3 Hz and longer. 3) The noise from the sky emission in the important "signal band" (determined by the speed the telescope moves over the source) is also apparent at frequencies between 1 and 10 Hz. 4) The response to the rectangular scan pattern we used can be seen as a feature at ~ 0.02 Hz (also picked up at lower level by the "dead" pixels, i.e. due to some mechanism for electric or magnetic coupling). It is interesting to note that the spike at ~ 5 minutes seen in the "dead pixel" average is likely to originate from oscillations of the ionosphere which are known to have resonance frequencies of a few minutes. 5) There are a significant number of noise spikes visible in the spectrum, the origin of most of which can be shown to being caused by a low number of fundamental frequencies (see Fig. 4). We are currently in the process of trying to identify the source of those noise spikes

V. Examples Of Astronomical Observations

A. Planet Observations

Figure 5 (left) shows an observation of the planet Mars, yielding a beam size of 21" x 15". The diffraction-limited resolution of the 30 m telescope at 2 mm wavelength is 15". This measurement represents the most extreme beam asymmetry; we made measurements of other point sources, which typically yielded beam sizes between 15" and 19".

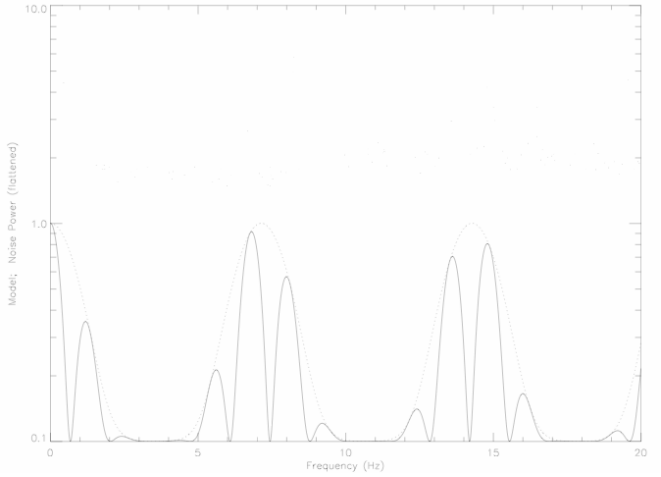

Fig.4 The dots show the flattened power spectrum with several clear sets of bands. The same data are displayed in all three panels, but on different frequency ranges. Some bands are strong enough that they extend beyond the top of the plot. The "model" spectrum indicated by the solid line is constructed from $\cos(\pi f / 1.352\ \mathrm{Hz})^2 \times [\mathrm{III}(7.142\ \mathrm{Hz}) \times e^{-0.5 f^2 / (1.59\ \mathrm{Hz})^2}] + 0.1$. The dotted line shows the envelope of the $\mathrm{III}(7.142\ \mathrm{Hz}) \times e^{-0.5 t^2 / (1.59\ \mathrm{Hz})^2}$ modulation

Figure 5 (right) shows the azimuthal beam shape in detail. No significant sidelobes are visible.

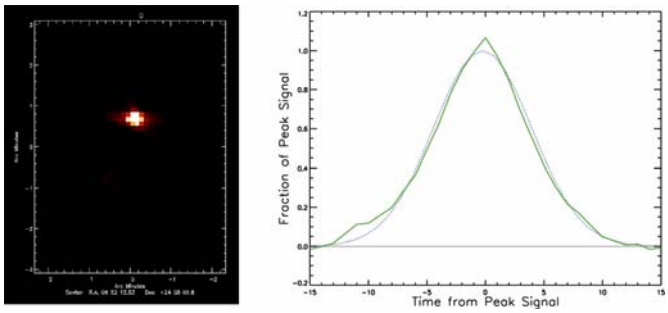

Fig. 5 *Left*: observation of the planet Mars. The fitted beam size is 21" x 15. This measurement represents the most extreme beam asymmetry we observed during measurements of point sources. *Right:* measured azimuthal beam shape derived from observations of Uranus (solid line), superimposed on a Gaussian distribution (dotted line)

B. Scan Patterns

Fig. 6 shows two typical scan patterns we used for observations: a) mapping by moving the telescope in azimuth (also called OTF mapping), and b) by alternating between mapping in azimuth and elevation directions (also called cross-linked OTF mapping). We soon abandoned the azimuth-only mapping, since the corresponding sky maps turned out to show residual spurious large scale structures. This can be understood by the fact that many areas of the sky in the azimuth-only maps will not have repeat observations in a sufficiently short period of time, and therefore the strong 1/*f*-like behavior of the atmosphere, seen in figure 3, does not allow a reliable estimate of the sky background. Both scan patterns were tested with and without chopping the telescope's secondary mirror. However, we did not discern

any benefit in using the chopper. Arbitrary scan patterns that allow each point of the sky to be revisited by a given pixel in a short amount of time, will optimize the achievable signal-to-noise ratio that one can achieve. An implementation of a Lissajous scanning pattern will be present at the 30m telescope by the time GISMO returns to the telescope in October of 2008. Another constraint to our observing efficiency for small maps suited to point sources was that there is a telescope drive software limit that does not allow the completion of an azimuth or elevation movement of the telescope in less than 10 seconds. The source signal for our smaller maps therefore was shifted toward lower frequencies than desired for optimum signal-to-noise performance of the observations. This problem will not affect us in the future with the implementation of the Lissajous mode, that is very well suited to mapping small areas.

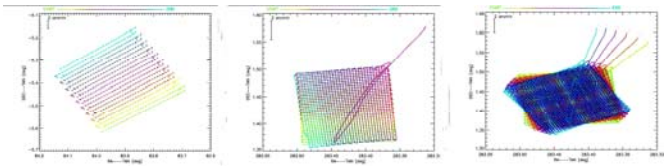

Fig. 6 Scan patterns used for our astronomical observations with the 30m telescope. *Left:* azimuthal scan pattern (OTF map). *Center:* azimuthal pattern, followed by scan pattern in elevation (cross linked OTF map). *Right*: Complete coverage for a 10 minute integration.Since the plots reflect the actual movement of the telescope which becomes obvious in the Az-El patterns shown here

C. *Astronomical Observations*

Figures 7 through 11 present a few examples of astronomical observations.

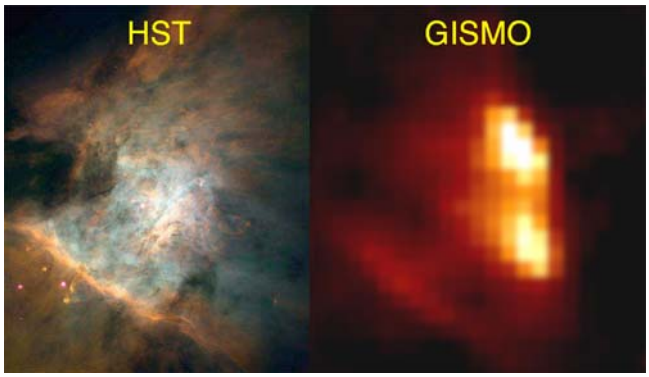

Fig. 7 HST imaged of the Orion Molecular Cloud. Right: GISMO's view of the same area. The integration time for this image was about 3 minutes

The software used to reduce the data shown in Figures 7 through 10 is a "quick view" package we have developed in order to be able to analyze the data during the observing run. Data for extended sources were high-pass filtered at 0.5 Hz, whereas those for point source observations had a point source Wiener filter (derived from GISMO Uranus images) applied. Then a fit to bolometer gains and offsets, based on the common time variations of the sky background, was applied to both data sets. Our first analysis indicates that with this preliminary data reduction package, a noise level a factor of about 3 above the atmospheric photon noise limit (which can be as low as 9 mJy/sqrt(s) under very good conditions) can be achieved for long integrations. The remaining excess noise is probably a combination of residual sky brightness variations and residual 1/*f* noise in the data, plus a constant background caused by the warm stop we were required to use during the first observing run as a result of our baffles being slightly undersized at that time.

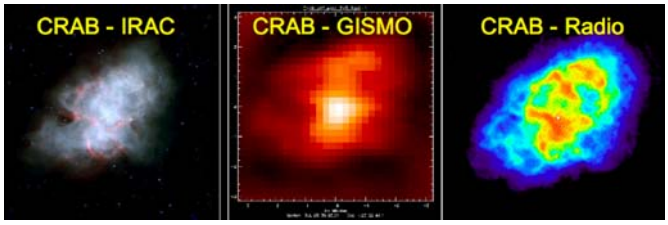

Fig. 8 The CRAB Nebula -- the result of a Supernova explosion – *(left)* in the infrared seen by the IRAC, *center* at 2mm as observed with GISMO, and *right* at centimeter wavelenghts as observed by the VLA

We have developed and are still in the process of improving a data reduction package that performs a least squares fit to the Fourier-transformed data. The algorithm is based on a scheme in which drift-dependent weights are applied to the data ("optimal mapping"). We are currently limited by the required computational resources, in that the memory use of the algorithm limits the amount of data for which we can compute a simultaneous solution. Fig. 10 shows an example of a 10 minute map of the Crab Nebula that was reduced with this package. The data shown here were downsampled by coadding into frames with an effective sampling rate of only 5 Hz.

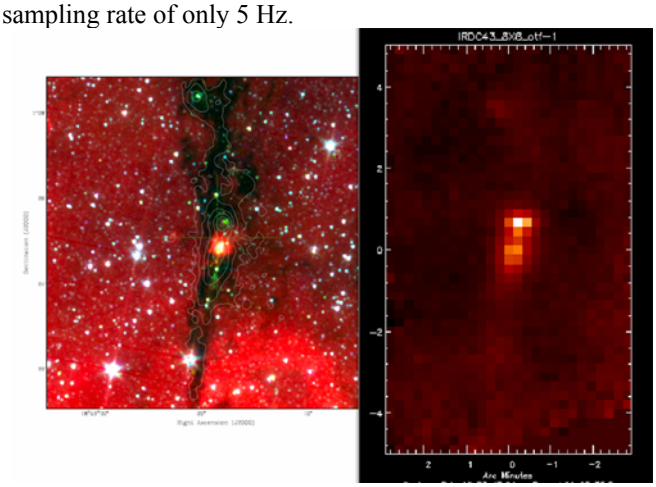

Fig. 9 *Left:* IRAC Glimpse N3-color IR image of the Infrared Dark Cloud IRDC43 with superimposed Mambo 1.2 mm contours (J. Jackson, priv. comm.). *Right:* GISMO's view of IRDC 43

We are working on the optimization of the code with respect to its requirement on computational resources. After further optimization we expect to have a data reduction pipeline available that will optimally extract the observed celestial flux from our astronomical targets.

CONCLUSION AND OUTLOOK

We have successfully fielded a 2mm TES bolometer camera at the IRAM 30 m telescope. We were able to obtain useful astronomical observations with a per-pixel sensitivity that was only a factor of about 3 above the expected, low, atmospheric photon noise at 2 mm.

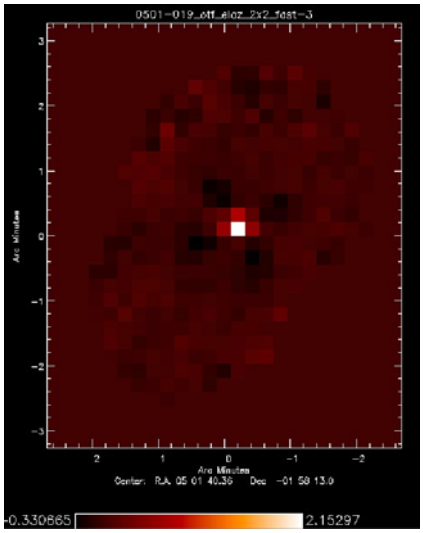

Fig. 10 The ~300 mJy quasar 0501-019 observed with a signal to noise ratio of 70

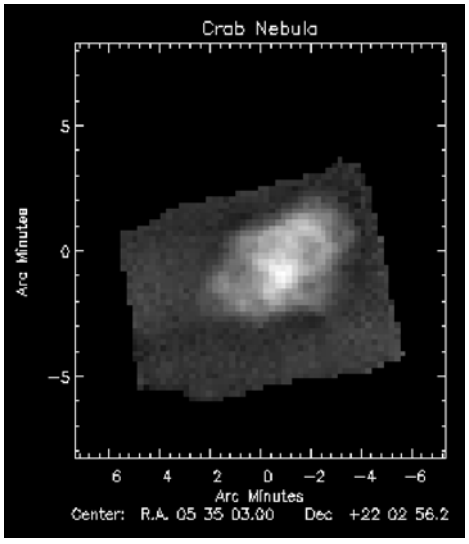

Fig. 11 Reduced map of a 10 minute integration on the Crab Nebula, reduced with our optimal weight method described in the text. The map appears to show more spatial frequencies than the map of Crab seen if Fig. 7, which we reduced with our quick look reduction software where we filtered our data by a 0.5 Hz highpass filter

We will return to the telescope later in 2008 with an improved baffling system and an improved mechanical design of the detector package. We are also building a shutter and illuminator for offset and gain calibration, and expect the introduction of a Lissajous scanning mode. With these enhancements, as well as our continued efforts to optimize our data reduction package, we expect a significantly improved performance of the instrument.

ACKNOWLEDGMENT

This work was supported in part by NSF Grant AST 0705185.

REFERENCES

[1] Baars, J. W. M., Hooghoudt, B. G.; Mezger, P. G.; de Jonge, M. J., 1983, A&A, 1785, 319

[2] de Korte, P.A. J., Beyer, J., Deiker, S., Hilton, G.C., Irwin, K.D., Macintosh, M., Nam, S.W., Reintsema, C.D., Vale, L. R., Huber, M.E., 2003, RScI, 74. 3807

[3] Staguhn, J. G.; Benford, D. J.; Allen, C.A.; Moseley, S. H.; Sharp, E. H.; Ames, T. J.; Brunswig, W.; Chuss, D. T.; Dwek, E.; Maher, S. F.; Marx, C. T.; Miller, T. M.; Navarro, S.; Wollack, E. J., "GISMO: a 2-millimeter bolometer camera for the IRAM 30 m telescope", 2006, SPIE, 6275E, 44S

[4] Allen, C. A., Benford, D. J., Miller, T. M., Moseley, S. H.; Staguhn, J. G.; Wollack, E. J., "Technology developments toward large format long wavelength bolometer arrays", 2007, SPIE, 6678, 4

[5] Staguhn, J.G., Dwek, E., Benford, D. J., Moseley, S.H., Sharp, E.H., "Science Case for a 2 mm Bolometer Camera Optimized for Surveys of Dusty Galaxies in the High Redshift Universe", Il Nuovo Cimento, in press.

[6] Bernstein, G., 2002, PASP, 114, 98

[7] Staguhn, J.G., Benford, D.J., Allen, C.A., Moseley, S.H., Sharp, E.H., Ames, T.J., Brunswig, W., Chuss, D.T., Dwek, E., Maher, S.F., Marx, C.T., Miller, T.M., Navarro, S., Wollack, E.J., "GISMO: a 2-millimeter bolometer camera for the IRAM 30 m telescope", 2006, SPIE, 6275E, 44S

[8] Dicker, S. R., Abrahams, J. A., Ade, P. A. R., Ames, T. J., Benford, D. J., Chen, T. C., Chervenak, J. A., Devlin, M. J., Irwin, K. D., Korngut, P. M., Maher, S., Mason, B. S., Mello, M., Moseley, S. H., Norrod, R. D., Shafer, R. A., Staguhn, J. G., Talley, D. J., Tucker, C., Werner, B. A., White, S. D., "A 90-GHz bolometer array for the Green Bank Telescope", 2006, SPIE, 6275E, 42D

[9] Allen, C. A.; Abrahams, J., Benford, D. J., Chervenak, J. A., Chuss, D. T., Staguhn, J. G., Miller, T. M., Moseley, S. H., Wollack, E. J., "Far infrared through millimeter backshort-under-grid arrays", 2006, SPIE, 6265E, 9A

[10] Staguhn, J.G., Benford, D.J., Chervenak, J.A., Moseley, S.H., Jr., Allen, C.A.; Stevenson, T.R.; Hsieh, W-T., ``Design techniques for improved noise performance of superconducting transition edge sensor bolometers", 2004, SPIE, 5498, 390

[11] Staguhn, J.G, Allen, C.A, Benford, D.J., Chervenak, J.A, Chuss, D.T., Miller, T.M., Moseley, S.H., Wollack, E.J., "Characterization of TES Bolometers used in 2-Dimensional Backshort-Under-Grid (BUG) Arrays for Far-Infrared Astronomy", 2006, Nuclear Instruments and Methods in Physics Research, Section A (NIMPA), 559, 545

[12] Kreysa, E., Gemünd, H.-P., Raccanelli, A., Reichertz, L. A. & Siringo, G., "Bolometer arrays for Mm/Submm astronomy", 2002, AIPC, 616, 262